14.14 USING TERRIAN ELEVATION INFORMATION TO IMPROVE THE QUALITY OF RADAR MOSAIC PRODUCTS

Joseph C. Lang*, Bradley D. Sutker, Gary S. Chase, Jiali Zhang
Unisys Weather Information Services, Kennett Square, Pennsylvania

1. INTRODUCTION

The quality of the data generated by the WSR-88D radars is adversely affected by many factors. These factors include: terrain features, the propagation path of the radar beam in the atmosphere, the presence of non-meteorological scatters in the atmosphere (e.g. birds, insects, dust, ash, chaff, etc.), RF interference, signal processing protocols, etc. The primary effects of terrain on radar data quality are unique in that they are relatively deterministic because terrain doesn't move. This paper describes the results-to-date of an on-going study being conducted by the Unisys Weather Information Services Group to investigate how terrain elevation data can be used to assess the quality of the data generated by the WSR-88D radars.

The majority of CONUS WSR-88D radars are sited at locations where terrain features extend into the volume of the atmosphere being scanned by the radar for some portion of the lower elevation tilts. There are two primary effects of these terrain features. The most significant effect is that the ability of the radar to "see" behind terrain obstructions is impaired. The second effect (which is generally not as significant) is the presence of persistent ground clutter returns that contaminate the radar products at the locations where terrain features extend into the path of the radar beam. As part of this study effort, techniques for generating terrain-based radar coverage maps and clutter maps have been developed and evaluated. This paper describes the models used for generating these maps, and describes the results of our evaluation of the correlation between these maps and radar product data. The evaluation of the accuracy of the terrain-based radar coverage and clutter maps indicates that they can be effectively utilized to assess the accuracy of radar product data.

The primary goal of this study is to develop improved algorithms that utilize these terrain-based radar coverage and clutter maps for generating more accurate radar mosaic products. At the time this paper is being prepared, this portion of the study has not yet been completed.

* Corresponding author address: Joseph C. Lang, Unisys Corporation, 221 Gale Lane, Kennett Square, PA 10348; e-mail: joseph.lang@unisys.com

Preliminary results of a mosaic algorithm that utilizes the radar coverage map information are described. The results to date are promising. We expect to have more conclusive results to report when the paper is presented at the Applications in Radar Session.

The terrain data used in this study was obtained from the National Imagery and Mapping Agency (NIMA). The data is generally known as DTED (Digital Terrain Elevation Data) Level 0. The DTED data is provided in a uniform matrix with a horizontal post spacing of 30 arc seconds (nominally one kilometer) and a terrain elevation resolution of one meter.

2. RADAR COVERAGE MAP MODEL

Figure 1 illustrates the model used for generating radar coverage maps for tilt 1 base reflectivity products. The model takes into account the effects of terrain blockage and earth curvature in computing radar coverage maps. Coverage maps are generated in radial format. For each one-degree azimuth sector of the product, the terrain elevation database is used to generate a terrain elevation profile as a function of distance from the radar along the radial. For each range bin along the radial, the elevations of the upper and lower edges of the one-degree pencil beam are computed using the 4/3 equivalent earth radius propagation model. For tilt 1 reflectivity products, the elevation angle of the lower edge of the beam is assumed to be 0 degrees, and the elevation angle of the upper edge of the beam is 1.0 degree.

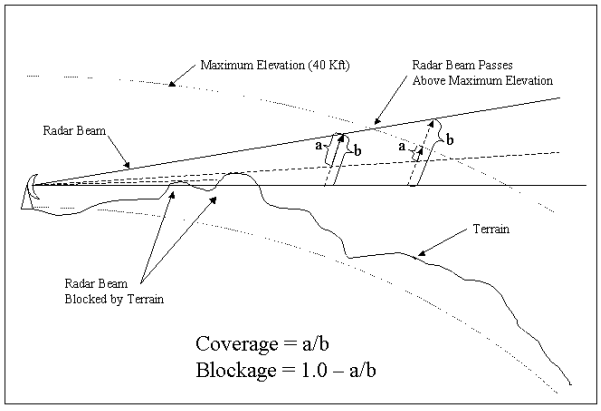

Figure 1. Radar Coverage Map Model for Base Reflectivity Products

Starting at the radar, radar coverage is computed for each range bin. The radar coverage takes into account the effects of both terrain obstructions between

the bin and the radar, and earth curvature. If the terrain elevation exceeds the elevation of the lower edge of the beam at any range ≤ the range of the bin, the beam is considered blocked by the terrain. In the far range of the product, due to earth curvature, the radar beam rises above the elevations where most of the weather occurs; coverage in these areas is considered reduced. For the coverage maps shown in this paper a maximum elevation of 40,000 ft was used. The radar coverage for a bin is computed as follows:

% Coverage = 100. * a / b

where:

a = Cross-sectional area of the beam above all terrain obstructions at ranges ≤ the range of the bin, and below the maximum elevation of interest

b = Total across – sectional area of the beam

Radial coverage functions decrease monotonically. Radar coverage decreases at ranges where terrain obstructions are encountered. Coverage remains at that level at ranges beyond the obstruction until/unless a higher terrain obstruction is encountered, or the beam begins to pass above the maximum elevation of interest. Although it is not shown in Figure 1, complete blockage occurs when the terrain elevation exceeds the elevation of the upper edge of the radar beam. Coverage at all ranges ≥ the range of the obstruction is considered to be 0%.

3. RADAR COVERAGE MAP EXAMPLES

Radar coverage maps were generated for 141 CONUS radar sites for the tilt 1 base reflectivity products. The coverage maps for 91 radars exhibit some degree of reduction in coverage due to the effects of terrain blockage. For 25 radars the effect is minimal, for 32 radars the effect is moderate, and for 34 radars the effect is significant. Coverage maps for 8 of the significantly impacted radars and 3 of the moderately impacted radars were evaluated against multi-hour sets of radar products collected for each radar under different weather conditions. The result of this evaluation demonstrated good correlation between the coverage maps and the product data. Several typical examples are shown below.

The coverage map for the tilt 1 base reflectivity product for the Albuquerque radar is shown in Figure 2. The gray areas indicate the regions of the product where coverage is degraded. The coverage map is displayed as a 10 level gray scale image. White areas indicate full coverage. The gray areas indicate regions of degraded coverage ranging from 90% coverage (lightest gray) to 0% coverage (darkest gray). The fans of degraded coverage arising in the vicinity of the radar are the result of terrain blockage. The map also shows rings of decreasing coverage in the far range as the radar beam passes through the 40,000 ft. elevation. The coverage map can also be interpreted as a blockage map with the white areas being regions of no blockage, the darkest gray areas being regions of complete blockage, and the intermediate gray areas being regions of partial blockage. The coverage map for the Albuquerque radar shows that the radar has full coverage only in the southwest quadrant and a 10-degree wedge to the northeast. There is degraded coverage due to terrain effects for approximately 270 degrees of the product. There is a thirty-degree wedge of complete blockage to the east, a smaller wedge of complete blockage to the west, and large regions of partial coverage in most of the product coverage area. Coverage changes rapidly with both range and azimuth.

In Figure 3, a product showing widespread showers moving from south to north is shown overlaid on the Albuquerque coverage map (the product and coverage map have been zoomed to show the area of interest). Weather returns moving through partially blocked areas fluctuate in amplitude consistent with the coverage level (note the southwest quadrant where the coverage fluctuates rapidly as a function of azimuth). Weather returns disappear abruptly as the weather moves into the blocked areas, and reappears abruptly as the weather emerges from the blocked areas.

Figure 4 shows a similar weather pattern overlaid on the coverage map for the Holloman AFB radar. This radar has an unobstructed view only in a 45 degree wedge to the south. There is a 135 degree wedge of complete blockage to the east, and a 180 degree wedge of fluctuating coverage to the west. The weather is widespread scattered showers moving from southwest to northeast. The weather in the partially obscured region to the southwest (where coverage varies in the range 10% - 90%) shows up as low amplitude rays (5-15 Dbz) at azimuths where the coverage level is higher. The returns disappear completely as the weather moves into the completely blocked area east of the radar. Figure 5 shows a second product generated one hour later when the weather in the partially blocked area in the southwest quadrant of Figure 4 has emerged into the unobstructed area of the product. The data levels have increased by 20-35 Dbz. Conversely, the weather returns in the unobstructed area in Figure 4 have completely disappeared into the completely blocked area in Figure 5.

The final coverage map example shown in Figure 6 is for the Burlington VT radar. This radar is situated in the Lake Champlain valley between the Adirondack and Green Mountains. The radar has relatively unobstructed coverage only to the north and south. The Figure shows a product containing a cluster of showers and thunderstorms moving northwest to southeast ahead of a front overlaid on the coverage map. Over a several hour period weather appeared abruptly as it emerged from the obstructed areas to the west and disappeared abruptly as it moved into the obstructed areas to the east. Note also that the weather fades away at far ranges where coverage decreases as the radar beam passes above the 40,000 foot elevation.

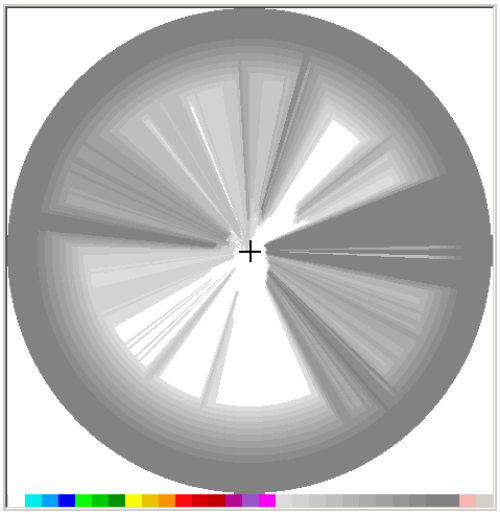

Figure 2. Radar Coverage Map for Albuquerque Radar

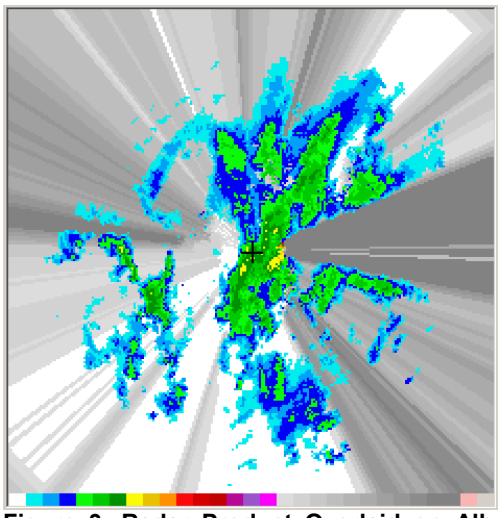

Figure 3. Radar Product Overlaid on Albuquerque Radar Coverage Map

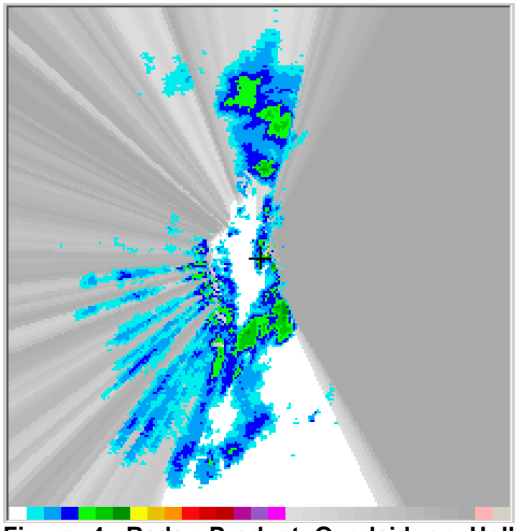

Figure 4. Radar Product Overlaid on Holloman AFB Radar Coverage Map

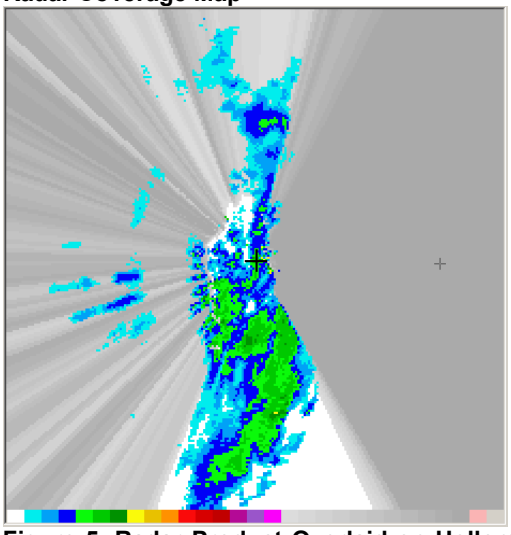

Figure 5. Radar Product Overlaid on Holloman AFB Radar Coverage Map (One hour later than Figure 4)

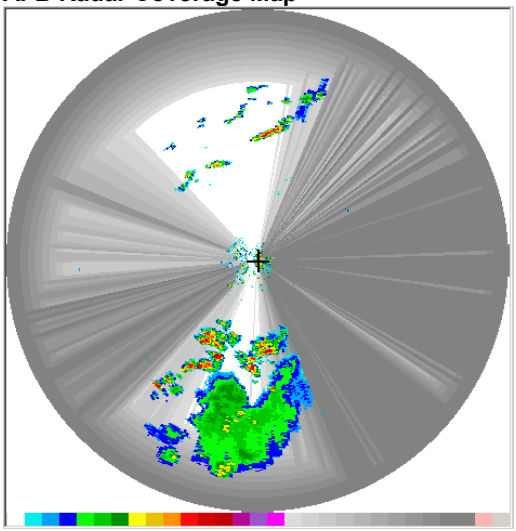

Figure 6. Radar Product Overlaid on Burlington VT Radar Coverage Map

4. RADAR CLUTTER MAP MODEL

Terrain elevation information can also be used to generate radar product clutter maps which identify areas of the product that may be impacted by the presence of persistent ground clutter returns. Figure 7 illustrates the model used for generating radar clutter maps for tilt 1 base reflectivity products.

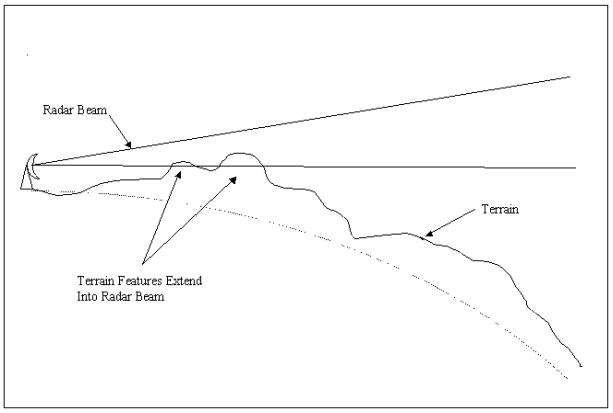

Figure 7. Clutter Map Model

This model is a simplified form of the coverage map model. Clutter maps are generated in radial format. For each one-degree azimuth sector of the product, the terrain elevation database is used to generate a terrain elevation profile as a function of distance from the radar along the radial. For each range bin along the radial, the elevation of the lower edge of the one-degree pencil beam (.0 degrees) is computed using 4/3 equivalent earth radius propagation model.

For each range bin of the radial, the terrain elevation is compared to the elevation of the lower edge of the radar beam at that range. If the terrain elevation exceeds the elevation of the lower edge of the beam for the bin, the corresponding bin in the clutter map is set to indicate possible clutter contamination.

After the clutter profiles have been computed for all 360 one-degree azimuth sectors, the 360 azimuth sectors are combined to create the clutter map. The map is then smeared slightly in both range and azimuth to broaden the clutter areas. The smearing helps account for the variations in the WSR-88D scanning strategies, the granularity of the terrain elevation data, and small deviations of the radar beam propagation path from the 4/3 equivalent earth radius propagation model path.

There is obviously a direct correlation between radar clutter maps and radar coverage maps generated from terrain elevation data. Clutter regions identified in the clutter maps are the result of terrain features which protrude into the radar beam, which in turn results in the blockage reflected in the radar coverage maps.

5. RADAR CLUTTER MAP EXAMPLES

The coverage map for the tilt 1 base reflectivity product for the Albuquerque radar is shown in Figure 8. Compare Figure 8 with the coverage map for this radar shown in Figure 2 (Figure 8 has been zoomed 2:1 to focus on the clutter regions which are in the near-range of the radar). The clutter areas correlate with the regions of the coverage map where the coverage levels decrease.

In Figure 9 a base reflectivity product generated under essentially clear air conditions is overlaid on the clutter map. This product was extracted from a series of products that showed the same data distribution pattern. As illustrated in Figure 9, these products contained small areas of isolated, stationary returns up to 45 Dbz that correlate very well with the clutter regions identified by the clutter map.

The WSR-88D radars have clutter-filtering capabilities that can be tailored to each radar site. In general, clutter filtering is only applied in range bins where it is needed. Clutter filtering can be enabled and disabled arbitrarily by the radar operators. The clutter-filtering regimen for a particular product is generally unknown to the users of the data. It is likely that clutter filtering was disabled at the time the product shown in Figure 9 was generated.

Compare the product in Figure 9 with the product shown in Figure 10, which is also overlaid on the clutter mask. This is a product from the same weather event shown in Figure 3 (30 minutes earlier). In contrast to the product shown in Figure 9, the product in Figure 10 does not contain the small patches of isolated high amplitude returns in the clutter regions (areas outlined by the red ellipses). Instead of high amplitude returns in these areas, this product contains “holes” in the data in these regions (the clutter mask in the background can be seen). These “holes” are more evident when a product loop of several hours is viewed. The “holes” remain stationary as the weather moves slowly from south to north over the clutter regions. The “holes” are also evident to a lesser degree in Figure 3.

It appears likely that at the time the products shown in Figures 3 and 10 were generated, clutter filtering was enabled. The “holes” in the products are the result of the clutter filters removing slow moving weather returns as well as clutter returns in the regions where clutter filtering was enabled.

In summary, terrain-based clutter maps can be used to identify regions of the product where the quality of the data may be degraded by the effects of clutter or clutter filtering.

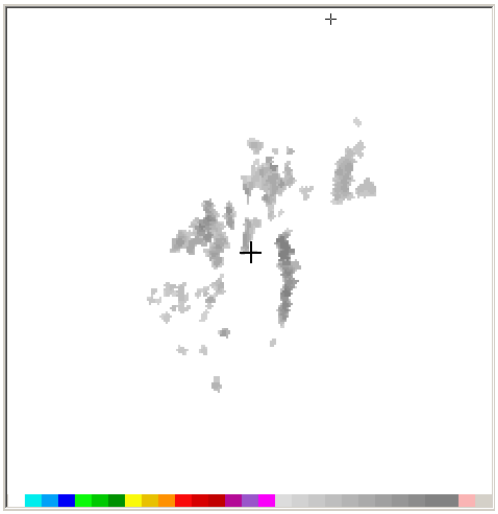

Figure 8. Clutter Map for the Albuquerque Radar

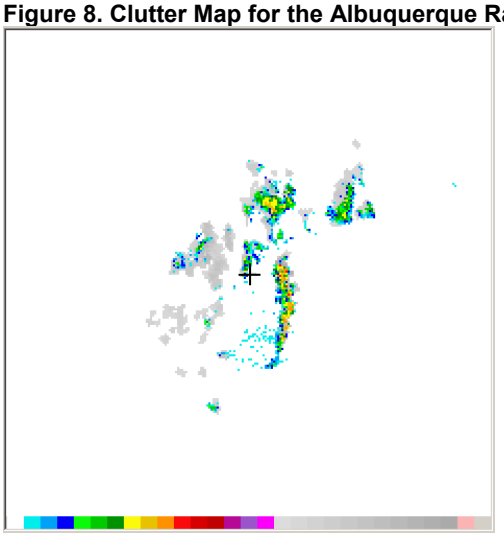

Figure 9. Radar Product Overlaid on the Albuquerque Clutter Map (Clutter Filtering is Probably Disabled)

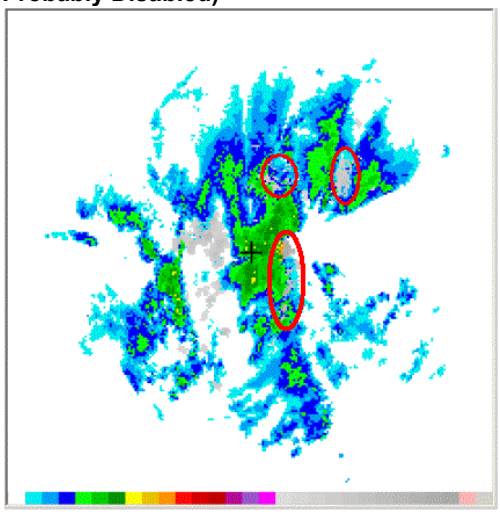

Figure 10. Radar Product Overlaid on the Albuquerque Clutter Map (Clutter Filtering is Probably Enabled)

6. APPLICATION OF TERRAIN INFORMATION IN RADAR MOSAIC ALGORITHMS

WSR-88D radar products may contain significant amounts of non-meteorological returns. As shown in the preceding discussion, radar products may also contain regions of missing or degraded weather data due to the effects of terrain blockage. The challenge in generating mosaic products from sets of overlapping radar products is to remove the non-meteorological content without distorting the weather content.

A most-likely contributor mosaic generation algorithm was developed for the FAA WARP program. For each mosaic bin, this algorithm assigns discrete confidence levels (high, medium, low) to each contributing radar bin. Confidence levels are based on the range of the contributing radar bin from its respective radar: near-range bins are assigned low confidence, mid-range bins are assigned high confidence, and far-range bins are assigned medium confidence. The contributing radar bins are sorted into confidence group subsets. Lower confidence data is discarded, and the mosaic bin value is then determined from the subset of contributors in the highest confidence group available using a highest supported contributor rule. This rule assigns the mosaic bin the value of the highest contributor in the subset of highest confidence contributors, provided that the difference between the highest contributor and the second highest contributor in the highest confidence group is $\leq$ a specified support level. If the support criterion is not met, the mosaic bin is assigned the value of the second highest contributor in the highest confidence group.

This most-likely contributor algorithm is quite effective in reducing the non-meteorological content of the mosaic products. However, in regions where terrain blockage is a significant factor, the algorithm also removes valid weather returns from the mosaic products. As a first step in utilizing terrain information in the mosaic generation process, the most-likely contributor algorithm was modified to use radar coverage map information as the basis for assigning contributing radar bins to a fourth confidence group, which is essentially "no confidence" data. Contributing radar bins that have radar coverage below a minimum level (radar coverage < 50% was used in the examples shown below) are assigned to the no confidence group, regardless of the range of the bin from its respective radar. Contributors that fall into the no confidence group are simply discarded. If there is no higher confidence data available for the mosaic bin, the mosaic bin is flagged as having no radar coverage.

In order to evaluate the effectiveness of this technique, data sets were collected and evaluated for several pairs of overlapping radars that have moderate to significant reductions in the overlap areas due to the effects of terrain blockage. Several examples are shown below.

The first example is a two-radar mosaic of tilt 1 base reflectivity products from the Burlington VT and Portland ME radars. The input products for the two radars overlaid on their respective radar coverage maps are shown in Figures 11 and 12. The Green and White Mountains in the overlap area result in reductions in radar coverage for both radars in the overlap area, particularly for the Burlington radar. The Burlington radar is unable to see the eastern half of the area of showers and thunderstorms to the south of the radar, which is where the strongest cells are located. In contrast, the Portland radar has a clear view of this region. The mosaic generated using the unmodified most-likely contributor algorithm is shown in Figure 13. The eastern portion of the area of showers and thunderstorms is missing from the mosaic because the corresponding bins in the completely blocked region of the Burlington radar product were treated as high confidence data. The mosaic bins in this region were mistakenly assigned the value of the data from the Burlington radar because the support criterion for the Portland radar data was not met. The mosaic generated using the terrain-enhanced most-likely contributor algorithm is shown in Figure 14. The eastern portion of the storm complex appears in the mosaic because the data from the Burlington radar in the blocked area has been discarded. Note the "no radar coverage" regions of the mosaic product (flat green areas), which identify the regions of the mosaic where there is no radar with coverage ≥ 50%.

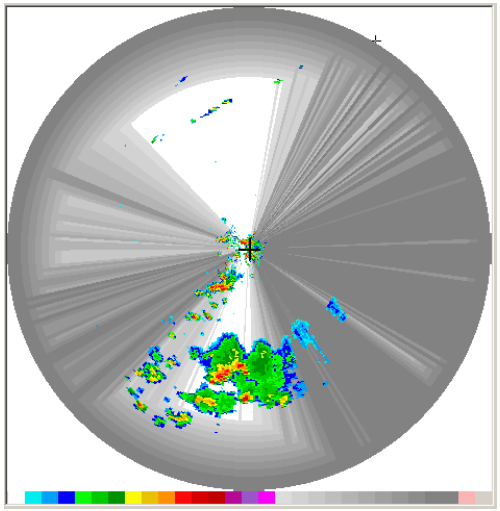

Figure 11. Radar Product Overlaid on the Burlington VT Radar Coverage Map

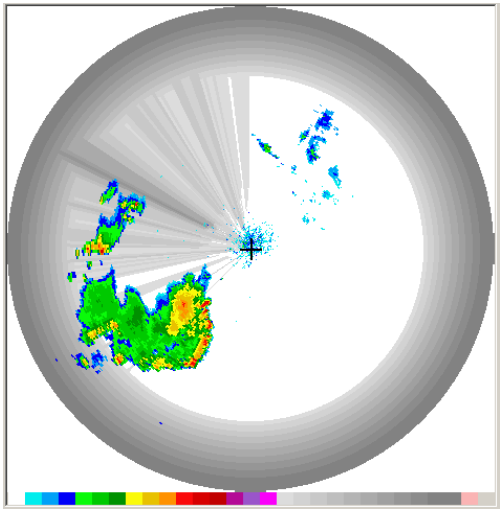

Figure 12. Radar Product Overlaid on the Portland ME Radar Coverage Map

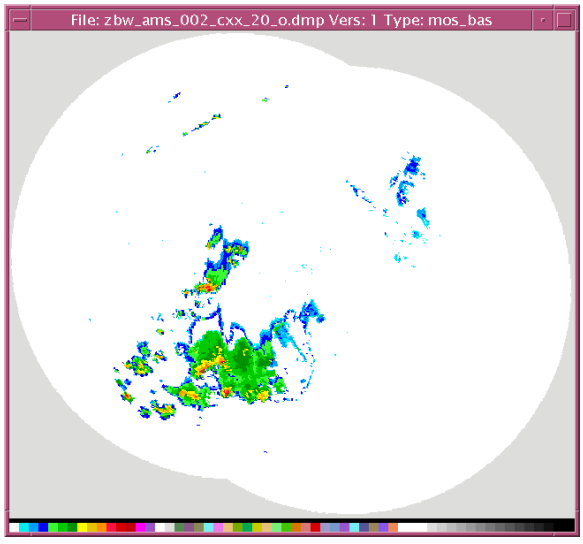

Figure 13. Burlington/Portland Mosaic Generated Using Unmodified Most-likely Contributor Algorithm

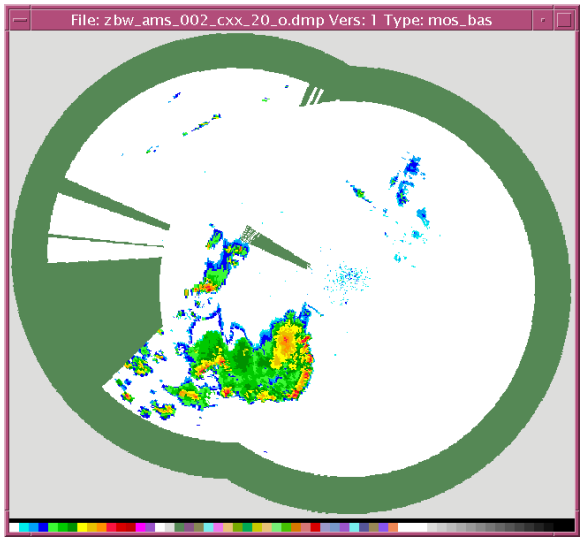

Figure 14. Burlington/Portland Mosaic Generated Using Terrain-enhanced Most-likely Contributor Algorithm

The second example is a two-radar mosaic of tilt 1 base reflectivity products from the Morristown TN and Greer SC radars. The input products for the two radars overlaid on their respective radar coverage maps are shown in Figures 15 and 16. The Smoky Mountains lie in the overlap area between the two radars. The products show a broad area of scattered showers and thunderstorms throughout most of the coverage areas of the two radars. The mosaic generated using the unmodified most-likely contributor algorithm is shown in Figure 17. Many storm features are missing from the mosaic as a result of terrain blockage. The mosaic generated using the terrain-enhanced most-likely contributor algorithm is shown in Figure 18. Most of the storm features are included in the mosaic. However, there are still some "holes" and reduced amplitude storm features that are the result of partial blockage (50% ≤ radar coverage < 100%).

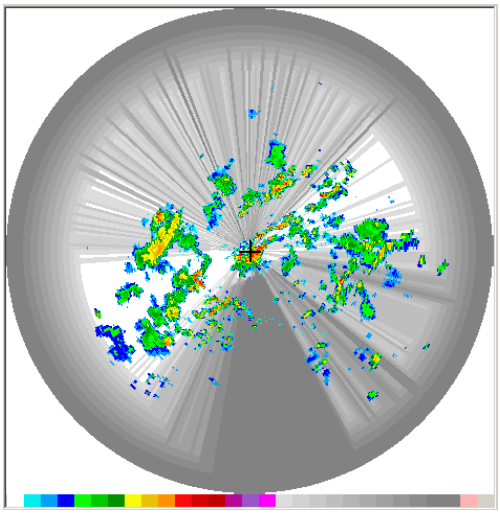

Figure 15 Radar Product Overlaid on the Morristown TN Radar Coverage Map

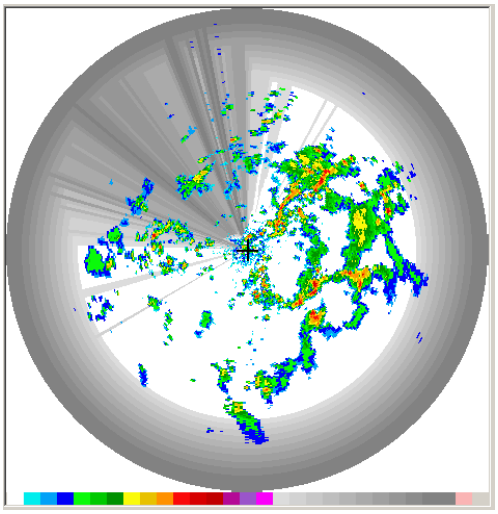

Figure 16. Radar Product Overlaid on the Greer SC Radar Coverage Map

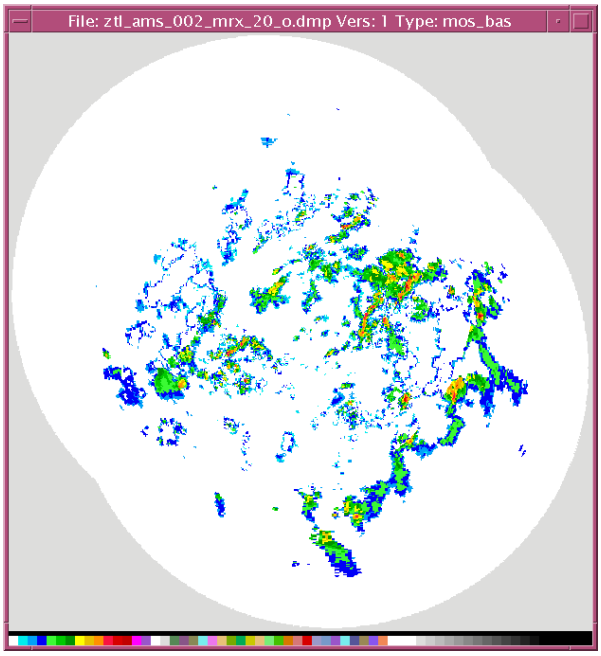

Figure 17. Morristown/Greer Mosaic Generated Using Unmodified Most-likely Contributor Algorithm

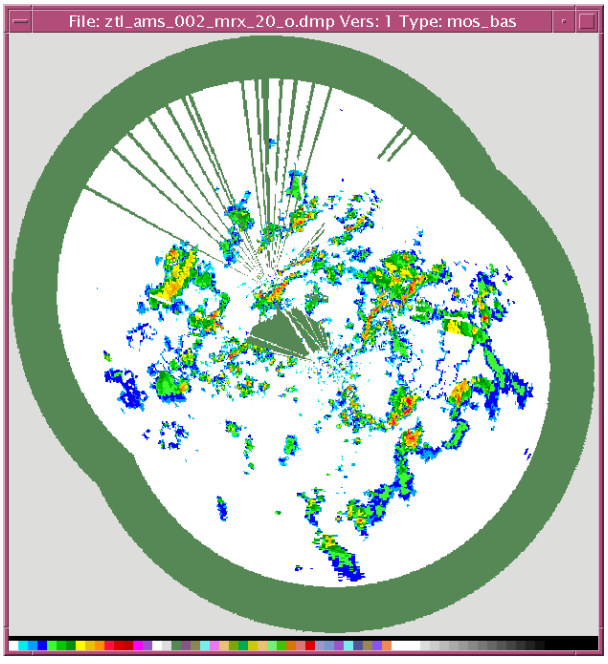

Figure 18. Morristown/Greer Mosaic Generated Using Terrain-enhanced Most-likely Contributor Algorithm

7.SUMMARY AND FUTURE WORK

Radar coverage maps generated from terrain elevation data correlate well with product data sets for the radars evaluated in this study. Radar coverage maps can be used to identify regions where weather returns may be degraded or missing as a result of terrain blockage. Clutter maps generated from terrain elevation data are also useful for identifying radar product regions where the data may be contaminated by the presence of persistent clutter returns. Preliminary study results indicate that radar coverage maps can also be used to improve the performance of mosaic generation algorithms. A study to investigate more sophisticated techniques for applying terrain-based radar coverage and clutter map information in mosaic generation algorithms is currently underway.